

## The landscape of host genetic factors involved in immune response to common viral infections

Linda Kachuri<sup>1\*</sup>, Stephen S. Francis<sup>1,2,3,4\*</sup>, Maïke Morrison<sup>5,6</sup>, George A. Wendt<sup>2</sup>, Yohan Bossé<sup>7</sup>, Taylor B. Cavazos<sup>8</sup>, Sara R. Rashkin<sup>1,9</sup>, Elad Ziv<sup>3,10,11</sup>, John S. Witte<sup>1,3,11,12</sup>

\* Authors contributed equally to this work

### Affiliations:

1. Department of Epidemiology and Biostatistics, University of California San Francisco, San Francisco, USA
2. Department of Neurological Surgery, University of California San Francisco, San Francisco, USA
3. Helen Diller Family Comprehensive Cancer Center, University of California, San Francisco, San Francisco, USA
4. Weill Institute for Neurosciences, University of California San Francisco, San Francisco, USA
5. Summer Research Training Program, Graduate Division, University of California San Francisco, San Francisco, USA
6. Department of Mathematics, The University of Texas at Austin, Austin, USA
7. Institut universitaire de cardiologie et de pneumologie de Québec, Department of Molecular Medicine, Université Laval, Quebec City, Canada
8. Program in Biological and Medical Informatics, University of California San Francisco, San Francisco, USA
9. Center for Applied Bioinformatics, St. Jude Children's Research Hospital, Memphis, USA
10. Department of Medicine, University of California, San Francisco, San Francisco, USA
11. Institute for Human Genetics, University of California San Francisco, San Francisco, USA
12. Department of Urology, University of California San Francisco, San Francisco, USA

### Corresponding Authors:

Stephen S. Francis

Department of Neurological Surgery  
Helen Diller Family Comprehensive Cancer Center  
University of California, San Francisco  
1450 3rd Street, Room 482, San Francisco, CA 94158  
Email: [stephen.francis@ucsf.edu](mailto:stephen.francis@ucsf.edu)

John S. Witte

Department of Epidemiology and Biostatistics  
Helen Diller Family Comprehensive Cancer Center  
University of California, San Francisco  
1450 3rd Street, Room 388, San Francisco, CA 94158  
Email: [jwitte@ucsf.edu](mailto:jwitte@ucsf.edu)

## ABSTRACT

**Introduction:** Humans and viruses have co-evolved for millennia resulting in a complex host genetic architecture. Understanding the genetic mechanisms of immune response to viral infection provides insight into disease etiology and therapeutic opportunities.

**Methods:** We conducted a comprehensive study including genome-wide and transcriptome-wide association analyses to identify genetic loci associated with immunoglobulin G antibody response to 28 antigens for 16 viruses using serological data from 7924 European ancestry participants in the UK Biobank cohort.

**Results:** Signals in human leukocyte antigen (HLA) class II region dominated the landscape of viral antibody response, with 40 independent loci and 14 independent classical alleles, 7 of which exhibited pleiotropic effects across viral families. We identified specific amino acid (AA) residues that are associated with seroreactivity, the strongest associations presented in a range of AA positions within DRβ1 at positions 11, 13, 71, and 74 for Epstein-Barr Virus (EBV), Varicella Zoster Virus (VZV), Human Herpes virus 7, (HHV7) and Merkel cell polyomavirus (MCV). Genome-wide association analyses discovered 7 novel genetic loci outside the HLA associated with viral antibody response ( $P < 5.0 \times 10^{-8}$ ), including *FUT2* (19q13.33) for human polyomavirus BK (BKV), *STING1* (5q31.2) for MCV, as well as *CXCR5* (11q23.3) and *TBKBP1* (17q21.32) for HHV7. Transcriptome-wide association analyses identified 114 genes associated with response to viral infection, 12 outside of the HLA region, including *ECSCR*:  $P = 5.0 \times 10^{-15}$  (MCV), *NTN5*:  $P = 1.1 \times 10^{-9}$  (BKV), and *P2RY13*:  $P = 1.1 \times 10^{-8}$  EBV nuclear antigen. We also demonstrated pleiotropy between viral response genes and complex diseases; from autoimmune disorders to cancer to neurodegenerative and psychiatric conditions.

**Conclusions:** Our study confirms the importance of the HLA region in host response to viral infection and elucidates novel genetic determinants beyond the HLA that contribute to host-virus interaction.

24     **KEY WORDS**

25     Infection, virus, serology, antigen, antibody, immunoglobulin G, immune response, human leukocyte  
26     antigen (HLA), polyomavirus, genome-wide association study (GWAS), transcriptome-wide association  
27     study (TWAS)

## INTRODUCTION

Viruses have been infecting cells for a half a billion years<sup>1</sup>. During our extensive co-evolution viruses have exerted significant selective pressure on humans and vice versa; overtly during fatal outbreaks, and covertly through cryptic immune interaction when a pathogen remains latent. The recent pandemic of severe acute respiratory syndrome coronavirus 2 (SARS-CoV-2) highlights the paramount public health need to understand human genetic variation in response to viral challenge. Clinical variation in COVID-19 severity and symptomatic presentation may be due to differences host genetic factors relating to immune response<sup>2</sup>. Furthermore, many common infections are cryptically associated with a variety of complex illnesses, especially those with an immunologic component, from cancer to autoimmune and neurologic conditions<sup>3-5</sup>. Despite their broad health relevance, few large-scale genome-wide association studies (GWAS) have been conducted on serological response phenotypes<sup>6-10</sup>. Understanding the genetic architecture of immunologic response to viruses may therefore provide new insight into etiologic mechanisms of diverse complex diseases.

Several common viruses exert a robust cell mediated and humoral immune response that bi-directionally modulate the balance between latent and lytic infection. Studies have demonstrated a strong heritable component (32-48%) of antibody response<sup>11</sup> and identified associations between host polymorphisms in genes relating to cell entry, cytokine production, and immune response and a variety of viruses<sup>12</sup>. The predominance of previously reported associations with have implicated genetic variants in human leucocyte antigen (HLA) class I and II genes in the modulation of immune response to diverse viral antigens<sup>7,13</sup>.

In this study we utilize data from the UK Biobank (UKB) cohort<sup>14</sup> to evaluate the relationship between host genetics and immunoglobulin G antibody response to 28 antigens for 16 viruses. Immunoglobulin G (IgG) antibody is the most common antibody in blood, which serves as a stable biomarker of lifetime exposure to common viruses. High levels of specific IgG's can be the result of chronic infection, while low levels may indicate poor immunity. Viruses assayed in the UKB multiplex serology panel were previously chosen based on putative links to chronic diseases including cancer, autoimmune, and neurodegenerative conditions<sup>15</sup>. We conduct integrative genome-wide and transcriptome-wide analyses of antibody response and positivity



to viral antigens (**Figure 1**), which elucidate novel genetic underpinnings of viral infection and immune response.

## METHODS

### *Study Population and Phenotypes*

The UK Biobank (UKB) is a population-based prospective cohort of over 500,000 individuals aged 40-69 years at enrollment in 2006-2010 who completed extensive questionnaires, physical assessments, and provided blood samples<sup>14</sup>. Analyses were restricted to individuals of predominantly European ancestry based on self-report and after excluding samples with any of the first two genetic ancestry principal components (PCs) outside of 5 standard deviations (SD) of the population mean (**Supplementary Figure 1**). We removed samples with discordant self-reported and genetic sex, samples with call rates <97% or heterozygosity >5 SD from the mean, and one sample from each pair of first-degree relatives identified using KING<sup>16</sup>.

Of the 413,810 European ancestry individuals available for analysis, a total of 7948 had serological measures. A multiplex serology panel (IgG) was performed over a 2-week period using previously developed methods<sup>17,18</sup> that have been successfully applied in epidemiological studies<sup>7,19</sup>. Details of the serology methods and assay validation performance are described in Mentzer et al.<sup>15</sup> Briefly, multiplex serology was performed using a bead-based glutathione S-transferase (GST) capture assay with glutathione-casein coated fluorescence-labelled polystyrene beads and pathogen-specific GST-X-tag fusion proteins as antigens<sup>15</sup>. Each antigen was loaded onto a distinct bead set and the beads were simultaneously presented to primary serum antibodies at serum dilution 1:1000<sup>15</sup>. Immunocomplexes were quantified using a Luminex 200 flow cytometer, which produced Median Fluorescence Intensities (MFI) for each antigen. The serology assay showed adequate performance, with a median coefficient of variation (CV) of 17% across all antigens and 3.5% among seropositive samples only<sup>15</sup>.

### *Genome-Wide Association Analysis*

We evaluated the relationship between genetic variants across the genome and serological phenotypes using PLINK 2.0 (October 2017 version). Participants were genotyped on the Affymetrix Axiom UK Biobank

array (89%) or the UK BiLEVE array (11%)<sup>14</sup> with genome-wide imputation performed using the Haplotype Reference Consortium data and the merged UK10K and 1000 Genomes phase 3 reference panels<sup>14</sup>. We excluded variants out of Hardy-Weinberg equilibrium at  $p < 1 \times 10^{-5}$ , call rate  $< 95\%$  (alternate allele dosage within 0.1 of the nearest hard call to be non-missing), imputation quality  $INFO < 0.30$ , and  $MAF < 0.01$ .

Seropositivity for each antigen was determined using established cut-offs based on prior validation work<sup>15</sup>. The primary GWAS focused on continuous phenotypes (MFI values), which measure the magnitude of antibody response, also referred to as seroreactivity. These analyses were conducted among seropositive individuals only for antigens with seroprevalence of  $\geq 20\%$  ( $n=1500$ ) based on 80% power to detect only common variants with large effect sizes at this sample size (**Supplementary Figure 2**). MFI values were transformed to standardized, normally distributed z-scores using ordered quantile normalization<sup>20</sup>.

Seroreactivity GWAS was conducted using linear regression with adjustment for age at enrollment, sex, body-mass index (BMI), socioeconomic status (Townsend deprivation index), the presence of any autoimmune and/or inflammatory conditions, genotyping array, serology assay date, quality control flag indicating sample spillover or an extra freeze/thaw cycle, and the top 10 genetic ancestry principal components (PC's). Autoimmune and chronic inflammatory conditions were identified using the following primary and secondary diagnostic ICD-10 codes (E10, M00-03, M05-M14, M32, L20-L30, L40, G35, K50-52, K58, G61) in Hospital Episode Statistics. Individuals diagnosed with any immunodeficiency (ICD-10 D80-89,  $n=24$ ) were excluded from all analyses.

For all antigens with at least 100 seropositive (or seronegative for pathogens with ubiquitous exposure) individuals, GWAS of discrete seropositivity phenotypes was undertaken using logistic regression, adjusting for the same covariates listed above.

The functional relevance of the lead GWAS loci for antibody response was assessed using in-silico functional annotation analyses based on Combined Annotation Dependent Depletion (CADD)<sup>21</sup> scores and RegulomeDB 2.0<sup>22</sup>, and by leveraging external datasets, such as GTEx v8, DICE (Database of Immune Cell Expression)<sup>23</sup>, and the Human Plasma Proteome Atlas<sup>24,25</sup>.

## Cross-Trait Associations with Disease

We explored pleiotropic associations between lead variants influencing antibody levels and several chronic diseases with known or hypothesized viral risk factors. Associations with selected cancers were obtained from a cancer pleiotropy meta-analysis of the UK Biobank and Genetic Epidemiology Research on Aging cohorts<sup>26</sup>. Summary statistics for the schizophrenia GWAS of 33,640 cases and 43,456 controls by Lam et al.<sup>27</sup> were downloaded from the Psychiatric Genomics Consortium. Association p-values were obtained from the National Institute on Aging Genetics of Alzheimer's Disease Data Storage Site for the GWAS by Jun et al.<sup>28</sup>, which included 17,536 cases and 53,711 controls. Associations with  $p < 7.3 \times 10^{-4}$  were considered statistically significant after correction for the number of variants and phenotypes tested.

## HLA Regional Analysis

For phenotypes displaying a genome-wide significant signal in the HLA region, independent association signals were ascertained using two complementary approaches: clumping and conditional analysis. Clumping is a post-processing step applied to GWAS summary statistics to identify independent association signals by grouping variants based on LD within specific windows. Clumping was performed on all variants with  $P < 5 \times 10^{-8}$  for each phenotype, as well as across phenotypes. Clumps were formed around index variants with the lowest p-value and all other variants with LD  $r^2 > 0.05$  within a  $\pm 500$  kb window were considered non-independent and assigned to that variant's clump.

Next, we conducted conditional analyses using a forward stepwise strategy to identify statistically independent signals within each type of variant (SNP/indel or classical HLA allele). Unlike clumping, conditional analyses involve fitting a new model that includes specific variants as covariates, thereby directly accounting for LD and providing association estimates that are adjusted for other relevant SNP effects. A total of 38,655 SNPs/indels on chromosome 6 (29,600,000 – 33,200,000 bp) were extracted to conduct regional analyses. Classical HLA alleles were imputed for UKB participants at 4-digit resolution using the HLA\*IMP:02 algorithm<sup>14</sup>, with modified settings to accommodate the addition of diverse samples from population reference panels described by Motyer et al.<sup>29</sup>. Details of the HLA imputation procedure are described in UKB Resource 182. Imputed dosages were available for 362 classical alleles in 11 genes:

*HLA-A*, *HLA-B*, and *HLA-C* (class I); *HLA-DRB5*, *HLA-DRB4*, *HLA-DRB3*, *HLA-DRB1*, *HLA-DQA1*, *HLA-DQB1*, *HLA-DPA1*, and *HLA-DPB1* (class II). Allele names with “99:01” for DRB3/4/5, which denote copy number absence, were renamed as “00:00” to avoid confusion with traditional HLA nomenclature. We also used SNP2HLA<sup>30</sup> to impute HLA alleles and corresponding amino acid sequences at a four-digit resolution in *HLA-A*, *HLA-B*, *HLA-C*, *HLA-DRB1*, *HLA-DQA1*, *HLA-DQB1*, *HLA-DPA1* and *HLA-DPB1* using the Type 1 Diabetes Genetics Consortium (T1DGC) reference panel comprised of 2,767 unrelated individuals of European descent. T1DGC was also among several reference datasets used by HLA\*IMP:02.

Analyses were restricted to common HLA alleles and amino acid sequences (frequency  $\geq 0.01$ ) with imputation quality scores  $>0.30$ , for a total of 1081 markers (101 alleles + 980 amino acid residues). Linear regression models were adjusted for the same set of covariates as the GWAS. Associations for each marker were considered statistically significant if  $P < 4.6 \times 10^{-5}$  based on Bonferroni correction for 1081 tests.

For each antigen response phenotype, we identified SNPs/indels or classical HLA alleles with the lowest p-value, among variants that achieved Bonferroni-significant associations ( $P < 4.6 \times 10^{-5}$ ), and performed forward iterative conditional regression to identify other independent signals, until no associations with a conditional p-value ( $P_{\text{cond}} < 5 \times 10^{-8}$ ) remained. We also assessed the independence of associations across different types of genetic variants by including conditionally independent HLA alleles as covariates in the SNP-based analysis.

For amino acid positions with  $>2$  possible residues (alleles), we applied the haplotype omnibus test to obtain an overall p-value for jointly testing all possible substitutions at that specific position. The omnibus test was applied to all amino acid residues at a given position, even if not all substitutions achieved the Bonferroni-corrected threshold ( $P < 4.6 \times 10^{-5}$ ) in the single-marker analysis. The frequency of amino acid substitutions at specific HLA alleles was determined using European ancestry reference populations part of the Allele Frequency Net Database (AFND 2020)<sup>31</sup>.

## Transcriptome-Wide Association Analysis

Gene transcription levels were imputed and analyzed using the MetaXcan approach<sup>32</sup>, applied to GWAS summary statistics for quantitative antigen phenotypes. For imputation, we used biologically informed MASHR-M prediction models<sup>33</sup> based on GTEx v8 with effect sizes computed using MASHR (Multivariate Adaptive Shrinkage in R)<sup>34</sup> for variants fine-mapped with DAP-G (Deterministic Approximation of Posteriors)<sup>35,36</sup>. An advantage of this approach is that MASHR effect sizes are smoothed by taking advantage of the correlation in cis-eQTL effects across tissues. For each antigen, we performed a transcriptome-wide association study (TWAS) using gene expression levels in whole blood. Statistically significant associations for each gene were determined based on Bonferroni correction for the number of genes tested.

We also examined gene expression profiles in tissues that represent known infection targets or related pathologies. Human herpesviruses and polyomaviruses are neurotropic and have been implicated in several neurological conditions<sup>37,38</sup>, therefore we considered gene expression in the frontal cortex. For Epstein-Barr virus (EBV) antigens additional models included EBV-transformed lymphocytes. Merkel cell polyomavirus (MCV) is a known cause of Merkel cell carcinoma<sup>39</sup>, a rare but aggressive type of skin cancer, therefore we examined transcriptomic profiles in skin tissues for MCV only.

Pathways represented by genes associated with antibody response to viral antigens were summarized by conducting enrichment analysis using curated Reactome gene sets and by examining protein interaction networks using the STRING database<sup>40</sup>. Significantly associated TWAS genes were grouped by virus family (herpesviruses vs. polyomaviruses) and specificity of association (multiple antigens vs. single antigen).

## RESULTS

A random sample of the participants representative of the full UKB cohort was assayed using a multiplex serology panel<sup>15</sup>. We analyzed data from 7924 participants of predominantly European ancestry, described in **Supplementary Table 1**. Approximately 90% of individuals were seropositive for herpes family viruses with ubiquitous exposure: EBV (EBV EA-D: 86.2% to ZEBRA: 91.2%), Human Herpesvirus 7 (HHV7 94.8%), and Varicella Zoster Virus (VZV 92.3%). Seroprevalence was somewhat lower for cytomegalovirus

(CMV), ranging between 56.5% (CMV pp28) and 63.3% (CMV pp52), and Herpes Simplex virus-1 (HSV1 69.3%). Human polyomavirus BKV was more prevalent (95.3%) compared to other polyomaviruses, Merkel cell polyoma virus (MCV 66.1%) and polyomavirus JC (JCV) (56.6%). Less common infections included HSV-2 (15.2%), HPV16 (E6 and E7 oncoproteins: 4.7%), HPV18 (2.4%), Human T-cell lymphotropic virus type 1 (HTLV1, 1.6%), Hepatitis B (HBV, 1.6%), and Hepatitis C (HCV, 0.3%).

### *Genetic Determinants of Response to Viral Infection*

Results from our GWAS of antibody response phenotypes were dominated by signals in the HLA region, which were detected for all EBV antigens (EA-D, EBNA, p18, ZEBRA), CMV pp52, HSV1, HHV7, VZV, JCV and MCV (**Table 1; Supplementary Figure 3**). Most of the top-ranking HLA variants for each antigen were independent of those for other antigens based on  $r^2$  but not D' (**Supplementary Figure 4**). Exceptions were moderate LD between lead variants for EBV ZEBRA and HSV1 ( $r^2=0.45$ ), EBV EBNA and JCV ( $r^2=0.45$ ), and HHV7 and MCV ( $r^2=0.44$ ). However, based on the complex LD structure and effect sizes, we cannot rule out that these linked to rare haplotypes. Outside of the HLA region, genome-wide significant associations with seroreactivity were detected for: MCV at 3p24.3 (rs776170649, *LOC339862*:  $P=1.7 \times 10^{-8}$ ) and 5q31.2 (rs7444313, *TMEM173* (also known as *STING1*):  $P=2.4 \times 10^{-15}$ ); BKV at 19q13.3 (rs681343, *FUT2*:  $P=4.7 \times 10^{-15}$ ) (**Figure 2**); EBV EBNA at 3q25.1 (rs67886110, *MED12L*:  $P=1.3 \times 10^{-9}$ ); HHV-7 at 11q23.3 (rs75438046, *CXCR5*:  $P=1.3 \times 10^{-8}$ ) and 17q21.3 (rs1808192, *TBKBP1*:  $P=9.8 \times 10^{-9}$ ); and HSV-1 at 10q23.3 (rs11203123:  $P=3.9 \times 10^{-8}$ ). However, the loci outside of HLA identified for HHV7 and HSV1 were not statistically significant considering a more stringent significance threshold corrected for the number of seroreactivity phenotypes tested ( $P < 5.0 \times 10^{-8}/16 = 3.1 \times 10^{-9}$ ).

GWAS of discrete seropositivity phenotypes identified associations in HLA for EBV EA-D (rs2395192: OR=0.66,  $P=4.0 \times 10^{-19}$ ), EBV EBNA (rs9268848: OR=1.60,  $P=1.2 \times 10^{-18}$ ), EBV ZEBRA (rs17211342: OR=0.63,  $P=1.6 \times 10^{-15}$ ), VZV (rs3096688: OR=0.70,  $P=3.7 \times 10^{-8}$ ), JCV (rs9271147: OR=0.54,  $P=1.3 \times 10^{-42}$ ), and MCV (rs17613347: OR=0.61,  $P=1.2 \times 10^{-26}$ ) (**Supplementary Figure 2; Supplementary Table 3**). An association with susceptibility to MCV infection was also observed at 5q31.2 (rs1193730215, *ECSCR*: OR=1.26,  $P=7.2 \times 10^{-9}$ ), with high LD ( $r^2=0.95$ ) between seroreactivity and seropositivity lead variants.

Several genome-wide significant associations were observed for antigens with <20% seroprevalence, which were not included in the GWAS of antibody response due to inadequate sample size (**Supplementary Table 3**). Infection susceptibility variants were identified for HSV2 in 17p13.2 (rs2116443: OR=1.28,  $P=4.5 \times 10^{-8}$ ; *ITGAE*); HPV16 E6 and E7 oncoproteins in 6p21.32 (rs601148: OR=0.60,  $P=3.3 \times 10^{-9}$ ; *HLA-DRB1*) and 19q12 (rs144341759: OR=0.383,  $P=4.0 \times 10^{-8}$ ; *CTC-448F2.6*); and HPV18 in 14q24.3 (rs4243652: OR=3.13,  $P=7.0 \times 10^{-10}$ ). Associations were also detected for Kaposi's sarcoma-associated herpesvirus (KSHV), HTLV1, HBV and HCV, including a variant in the *MERTK* oncogene (HCV Core rs199913364: OR=0.25,  $P=1.2 \times 10^{-8}$ ). After correcting for 28 serostatus phenotypes tested ( $P < 1.8 \times 10^{-9}$ ), the only statistically significant associations remained for EBV EA-D (rs2395192), EBV EBNA (rs9268848), EBV ZEBRA (rs17211342), JCV (rs9271147), MCV (rs17613347), and HPV18 (rs4243652).

#### *Functional Characterization of GWAS Findings*

In-silico functional analyses of the lead 17 GWAS variants identified enrichment for multiple regulatory elements (summarized in **Supplementary Table 4**). Three variants were predicted to be in the top 10% of deleterious substitutions in GRCh37 based on CADD scores >10: rs776170649 (MCV, CADD=15.61), rs139299944 (HHV7, CADD=12.15), and rs9271525 (JCV, CADD=10.73). Another HHV7-associated variant, rs1808192 (RegulomeDB rank: 1f), an eQTL and sQTL for *TBKBP1*, mapped to 44 functional elements for multiple transcription factors, including IKZF1, a critical regulator of lymphoid differentiation frequently mutated in B-cell malignancies.

Eleven sentinel variants were eQTLs and 8 were splicing QTLs in GTEx, with significant ( $FDR < 0.05$ ) effects across multiple genes and tissues (**Supplementary Figure 5**). The most common eQTL and sQTL targets included *HLA-DQA1*, *HLA-DQA2*, *HLA-DQB1*, *HLA-DQB2*, *HLA-DRB1*, and *HLA-DRB6*. Outside of HLA, rs681343 (BKV), a synonymous *FUT2* variant was an eQTL for 8 genes, including *FUT2* and *NTN5*. MCV variant in 5q31.2, rs7444313, was an eQTL for 7 genes, with concurrent sQTL effects on *TMEM173*, also known as *STING1* (stimulator of interferon response cGAMP interactor 1) and *CXXC5*. Gene expression profiles in immune cell populations from DICE<sup>23</sup> identified several cell-type specific effects that were not observed in GTEx. An association with *HLA-DQB1* expression in CD4<sup>+</sup> T<sub>H</sub>2 cells was observed for



rs9273325, 6:31486158\_GT\_G was an eQTL for *ATP6V1G2* in naïve CD4<sup>+</sup> T cells, and rs1130420 influenced the expression of 8 HLA class II genes in naïve B-cells and CD4<sup>+</sup> T<sub>H</sub>17 cells.

We identified 7 significant ( $p < 5.0 \times 10^{-8}$ ) protein quantitative trait loci (pQTL) for 38 proteins (**Supplementary Table 5**). Most of the pQTL targets were components of the adaptive immune response, such as the complement system (C4, CFB), chemokines (CCL15, CCL25), and defensin processing (Beta-defensin 19, Trypsin-3). The greatest number and diversity of pQTL targets ( $n=16$ ) was observed for rs681343, including BPIFB1, which plays a role in antimicrobial response in oral and nasal mucosa<sup>41</sup>; FUT3, which catalyzes the last step of Lewis antigen biosynthesis; and FGF19, part of the PI3K/Akt/MAPK signaling cascade that is dysregulated in cancer and neurodegenerative diseases<sup>42</sup>.

#### *Cross-trait associations with disease outcomes*

To contextualize the relevance of genetic loci involved in infection response, we explored associations with selected cancers, schizophrenia, and that have a known or suspected viral etiology (**Supplementary Table 6**). The strongest secondary signal was observed for rs9273325 (*HLA-DQB1*), which was negatively associated with VZV antibody response and positively associated with schizophrenia susceptibility (OR=1.13,  $P=4.3 \times 10^{-15}$ ). Other significant (Bonferroni  $P < 7.4 \times 10^{-4}$ ) associations with schizophrenia were detected for HSV1 (rs1130420: OR=1.06,  $P=1.8 \times 10^{-5}$ ), EBV EA-D (rs2647006: OR=0.96,  $P=2.7 \times 10^{-4}$ ), JCV (rs9271525: OR=1.06,  $P=6.8 \times 10^{-5}$ ) and BKV (rs681343: OR=0.96,  $P=2.5 \times 10^{-4}$ ), with the latter being the only pleiotropic signal outside of HLA. Inverse associations with hematologic cancers were observed for HSV1 (rs1130420: OR=0.89,  $P=3.5 \times 10^{-6}$ ), VZV (rs9273325: OR=0.88,  $P=4.4 \times 10^{-5}$ ), and EBV EBNA (rs9269233: OR=0.88,  $P=2.7 \times 10^{-4}$ ) variants. HSV1 antibody response was also linked to Alzheimer's disease (rs1130420:  $P=1.2 \times 10^{-4}$ ).

#### *Regional HLA Associations*

Associations within the HLA region were refined by identifying independent (LD  $r^2 < 0.05$  within  $\pm 500$ kb) index variants with  $P < 5.0 \times 10^{-8}$  for each antigen response phenotype (**Supplementary Table 7**). Clumping seropositivity associations with respect to lead antibody response variants did not retain any loci,



suggesting non-independence in signals for infection and reactivity for the same antigen. For this reason, all subsequent analyses focus on seroreactivity phenotypes. Clumping across phenotypes to assess the independence of HLA associations for different antigens identified 40 independent index variants: EBV EBNA (12), VZV (11), EBV ZEBRA (8), EBV p18 (5), MCV (3), and EBV EA-D (1) (**Supplementary Table 9**). No LD clumps were anchored by variants detected for CMV pp52, HHV7, HSV1, or JCV, suggesting that the HLA signals for these antigens are captured by lead loci for other phenotypes. The largest region with the lowest p-value was anchored by rs9274728 ( $P=4.7\times 10^{-67}$ ) near *HLA-DQB1*, originally detected for EBV ZEBRA. Of the 11 VZV-associated variants, the largest clump was formed around rs4990036 ( $P=4.5\times 10^{-26}$ ) in *HLA-B*.

Iterative conditional analyses adjusting for the HLA SNP/indel with the lowest p-value were performed until no variants remained with  $P_{\text{cond}} < 5.0\times 10^{-8}$ . Additional independent variants were identified for EBV EBNA (rs139299944, rs6457711, rs9273358, rs28414666, rs3097671), EBV ZEBRA (rs2904758, rs35683320, rs1383258), EBV p18 (rs6917363, rs9271325, rs66479476), and MCV (rs148584120, rs4148874) (**Figure 3; Supplementary Table 8**). For CMV pp52, HHV7, HSV1, JCV, and VZV, the regional HLA signal was captured by the top GWAS variant (**Figure 2; Supplementary Table 8**).

Next, we tested 101 classical HLA alleles and performed analogous iterative conditional analyses for significantly associated variants ( $P < 4.6\times 10^{-5}$ ). To help with the interpretation of our results, we depict the LD structure for HLA alleles in class II genes in **Supplementary Figure 5**. Significant associations across viruses were predominantly observed for class II HLA alleles. Five statistically independent signals were identified for antibody response to EBV ZEBRA (DRB4\*00:00:  $\beta = -0.246$ ,  $P = 1.4\times 10^{-46}$ ; DQB1\*04:02:  $\beta_{\text{cond}} = 0.504$ ,  $P_{\text{cond}} = 1.0\times 10^{-19}$ ; DRB1\*04:04:  $\beta_{\text{cond}} = 0.376$ ,  $P_{\text{cond}} = 1.1\times 10^{-18}$ ; DQA1\*02:01:  $\beta_{\text{cond}} = 0.187$ ,  $P_{\text{cond}} = 1.1\times 10^{-10}$ , A\*03:01:  $\beta_{\text{cond}} = 0.129$ ,  $P_{\text{cond}} = 1.9\times 10^{-8}$ ) (**Figure 3; Supplementary Table 11**). DRB4\*00:00 represents copy number absence, which co-occurs with DRB1\*04 and DRB1\*07 alleles<sup>43</sup>. This is consistent with the magnitude and direction of unconditional associations observed for DRB1\*07:01 ( $\beta = 0.251$ ,  $P = 1.3\times 10^{-26}$ ) and DRB4\*04:01 ( $\beta = 0.293$ ,  $P = 7.9\times 10^{-22}$ ). Five conditionally independent alleles were also identified for EBV EBNA: DRB5\*00:00:  $\beta = -0.246$ ,  $P = 8.7\times 10^{-30}$ ; DRB3\*02:02:  $\beta_{\text{cond}} = 0.276$ ,  $P_{\text{cond}} = 6.8\times 10^{-30}$ ; DQB1\*02:01:  $\beta_{\text{cond}} = -0.164$ ,  $P_{\text{cond}} = 3.6\times 10^{-12}$ ; DRB4\*00:00:  $\beta = 0.176$ ,  $P_{\text{cond}} = 8.3\times 10^{-17}$ ; DPB1\*03:01:  $\beta_{\text{cond}} = -$

0.220,  $P_{\text{cond}}=4.7 \times 10^{-14}$  (**Figure 3; Supplementary Table 11**). DRB5\*00:00 denotes a copy number deletion that sits on an common haplotype comprised of DRB1\*15:01, DQB1\*06:02, DQA1\*01:02<sup>43</sup>, which may also include DRB5\*01:01<sup>44</sup> (**Supplementary Figure 6**). The presence of the DRB1\*15:01-DQB1\*06:02-DQA1\*01:02 haplotype was associated with increased EBV EBNA seroreactivity ( $\beta=0.330$ ,  $P=2.5 \times 10^{-28}$ ). Fewer independent alleles were observed for EBV p18 (DRB5\*00:00:  $\beta=-0.210$ ,  $P=1.7 \times 10^{-22}$ ; DRB1\*04:04:  $\beta_{\text{cond}}=0.357$ ,  $P_{\text{cond}}=1.3 \times 10^{-18}$ ) (**Figure 3; Supplementary Tables 12**).

DQB1\*02:01 was the only independently associated allele for EBV EA-D ( $\beta=-0.154$ ,  $P=8.4 \times 10^{-11}$ ) and HSV1 ( $\beta=0.145$ ,  $P=2.8 \times 10^{-8}$ ), although its effects were in opposite directions for each antigen (**Supplementary Table 13**). For VZV, associations with 16 classical alleles were accounted for by DRB1\*03:01 ( $\beta=0.236$ ,  $P=7.3 \times 10^{-26}$ ). JCV shared the same lead allele as EBV EBNA and EBV p18 (DRB5\*00:00:  $\beta=0.350$ ,  $P=1.2 \times 10^{-21}$ ) (**Supplementary Table 13**). Four conditionally independent signals were identified for MCV (DQA1\*01:01:  $\beta=0.215$ ,  $P=1.1 \times 10^{-15}$ ; DRB1\*04:04:  $\beta_{\text{cond}}=-0.362$ ,  $P_{\text{cond}}=3.0 \times 10^{-11}$ ; A\*29:02:  $\beta_{\text{cond}}=-0.350$ ,  $P=1.0 \times 10^{-11}$ ; DRB1\*15:01:  $\beta_{\text{cond}}=-0.203$ ,  $P=3.7 \times 10^{-12}$ ) (**Figure 3; Supplementary Table 14**). Lastly, we integrated associations across variant types by including conditionally independent HLA alleles as covariates in the SNP-based analysis. With the exception of EBV antigens and HHV7, classical HLA alleles captured all genome-wide significant SNP signals (**Supplementary Figure 7**).

Finally, we tested 980 HLA amino acid substitutions (**Supplementary Tables 15-24**), followed by omnibus haplotype tests at each position that had a significant amino acid and more than two possible alleles. The strongest allele-specific and haplotype associations were found at different positions in the same protein for EBV p18 (DR $\beta$ 1 Ala -17:  $\beta=-0.194$ ,  $P=1.0 \times 10^{-21}$ ; DR $\beta$ 1 (13):  $P_{\text{omni}}=4.6 \times 10^{-22}$ ), MCV (DQ $\beta$ 1 Leu-26:  $\beta=-0.173$ ,  $P=7.0 \times 10^{-18}$ ; DQ $\beta$ 1 (125):  $P_{\text{omni}}=2.0 \times 10^{-17}$ ), HHV7 (DQ $\beta$ 1 His-30:  $\beta=-0.111$ ,  $P=1.2 \times 10^{-8}$ ; DQ $\beta$ 1 (57):  $P_{\text{omni}}=5.6 \times 10^{-9}$ ), and HHV6 IE1B at (DR $\beta$ 1 Ile-67:  $\beta=0.131$ ,  $P=1.6 \times 10^{-8}$ ; DR $\beta$ 1 (13):  $P_{\text{omni}}=1.1 \times 10^{-5}$ ).

The strongest residue-specific and haplotype associations mapped to the same amino acid position for four phenotypes: EBV ZEBRA (**Supplementary Table 18**), HHV6 IE1A (**Supplementary Table 19**), HSV1 (**Supplementary Table 21**), and JCV (**Supplementary Table 23**). Amino acid residues at DQ $\alpha$ 1 (175) were associated with antibody response to EBV ZEBRA (Glu:  $\beta=0.279$ ,  $P=1.1 \times 10^{-61}$ ;  $P_{\text{omni}}=8.3 \times 10^{-62}$ ). Glu-175 is

present in DQA1\*02:01 ( $P=4.9\times 10^{-27}$ ), DQA1\*03:01 ( $P=1.3\times 10^{-16}$ ), DQA1\*04:01 ( $P=1.9\times 10^{-12}$ ), and seems to better summarize the EBV ZEBRA signal at this locus. Substitutions in DR $\beta$ 1 (96) contained the strongest predictors of JCV seroreactivity (His or Tyr:  $\beta=0.325$ ,  $P=1.6\times 10^{-25}$ ;  $P_{\text{omni}}=7.7\times 10^{-23}$ ). His-96/Tyr-96 are in high LD ( $r^2=0.92$ ) with DRB5\*00:00, the top JCV-associated allele. However, this might mask the signal for Gln-96 ( $\beta=-0.310$ ,  $P=9.0\times 10^{-23}$ ), which is part of the DRB1\*15:01 sequence ( $\beta=-0.309$ ,  $P=9.0\times 10^{-21}$ ; LD  $r^2=0.94$ ). The lead signal for HSV1 mapped to DQ $\beta$ 1 (57) (Ala:  $\beta=0.123$ ,  $P=2.2\times 10^{-10}$ ;  $P_{\text{omni}}=6.5\times 10^{-9}$ ), which aligns with the association for the lead HSV1-allele DQB1\*02:01.

For EBV EBNA the strongest haplotype association was in DR $\beta$ 1 (37) ( $P_{\text{omni}}=1.1\times 10^{-55}$ ), while the residue with the lowest p-value was DQ $\beta$ 1 Ala-57 ( $\beta=-0.237$ ,  $P=1.4\times 10^{-42}$ ) (**Supplementary Table 16**). Ala-57 maps to multiple DQB1 alleles and achieved a stronger signal for EBV EBNA than any classical HLA allele. Asp-9 in HLA-B showed the strongest association with antibody response to EBV EA-D ( $\beta=-0.146$ ,  $P=1.8\times 10^{-9}$ ; **Supplementary Table 15**) and VZV ( $\beta=0.237$ ,  $P=9.7\times 10^{-25}$ ; **Supplementary Table 22**). This amino acid sequence is part of B\*08:01, which had analogous effects on both phenotypes (EBV EA-D:  $\beta=-0.144$ ,  $P=2.7\times 10^{-9}$ ; VZV:  $\beta=0.238$ ,  $P=4.7\times 10^{-25}$ ). Haplotypes with the lowest overall p-values were found in DQ $\beta$ 1 (71) for VZV ( $P_{\text{omni}}=9.8\times 10^{-19}$ ) and DR $\beta$ 1 (11) for EBV EA-D ( $P_{\text{omni}}=1.7\times 10^{-10}$ ).

### *TWAS of Genes Involved in Antibody Response*

Based on known targets of infection or related pathologies, we considered expression in the frontal cortex (**Supplementary Table 25**), EBV-transformed lymphocytes for EBV antigens (**Supplementary Table 26**), and skin for MCV (**Supplementary Table 27**). Concordance across tissues was summarized using Venn diagrams (**Figure 4**; **Supplementary Figure 8**). TWAS identified 114 genes significantly associated ( $P_{\text{TWAS}}<4.2\times 10^{-6}$ ) with antibody response in at least one tissue, 54 of which were associated with a single phenotype, while 60 influenced seroreactivity to multiple antigens. We also include results for 87 additional suggestively ( $P_{\text{TWAS}}<4.2\times 10^{-5}$ ) associated genes.

The TWAS results included a predominance of associations in HLA class II genes. Some of the strongest overall associations were observed for *HLA-DRB5* (EBV ZEBRA:  $P_{\text{cortex}}=4.2\times 10^{-45}$ ) and *HLA-DRB1* (EBV EBNA:  $P_{\text{cortex}}=6.7\times 10^{-39}$ ; EBV ZEBRA:  $P_{\text{cortex}}=3.3\times 10^{-33}$ ; JCV:  $P_{\text{cortex}}=6.5\times 10^{-14}$ ; EBV p18:  $P_{\text{cortex}}=2.2\times 10^{-12}$ ).

Increased expression of *HLA-DQB2* was positively associated with antibody response to EBV ZEBRA ( $P_{\text{blood}}=7.6\times10^{-19}$ ), JCV ( $P_{\text{blood}}=9.9\times10^{-10}$ ), VZV ( $P_{\text{blood}}=7.0\times10^{-9}$ ), HHV7 ( $P_{\text{blood}}=7.3\times10^{-8}$ ), and HSV1 ( $P_{\text{blood}}=3.3\times10^{-7}$ ), but negatively associated with EBV EBNA ( $P_{\text{blood}}=3.6\times10^{-34}$ ) and EBV p18 ( $P_{\text{blood}}=2.1\times10^{-8}$ ), in a consistent manner across tissues. The opposite was observed for *HLA-DQB1*, with positive effects on EBV EBNA and EBV p18 and inverse associations with EBV ZEBRA, JCV, VZV, HHV7, and HSV1.

The TWAS analyses also identified a number of significant associations in the HLA class III region that were not detected in other analyses. The top-ranking VZV associated gene was *APOM* ( $P_{\text{blood}}=7.5\times10^{-27}$ ,  $P_{\text{cortex}}=1.1\times10^{-25}$ ). Interestingly, opposite directions of effect were observed for *C4A* and *C4B* gene expression. Increased *C4A* expression was positively associated with all EBV antigens (**Supplementary Table 26**), but negatively associated with VZV ( $P_{\text{blood}}=2.3\times10^{-24}$ ) and HSV1 ( $P_{\text{cortex}}=1.8\times10^{-5}$ ) antibody levels (**Supplementary Table 25**). On the other hand, increased *C4B* expression was inversely associated with EBV phenotypes, but positively associated with VZV ( $P_{\text{blood}}=8.1\times10^{-25}$ ) and HSV1 ( $P_{\text{blood}}=1.1\times10^{-5}$ ). A similar pattern was also observed for *CYP21A2* and *C2*, with positive effects on antibody response to VZV and HSV1, and negative effects for all EBV antigens. Other novel TWAS findings were detected for HHV7 in 22q13.2 (*CTA-223H9.9*:  $P_{\text{TWAS}}=2.5\times10^{-6}$ ; *CSDC2*:  $P_{\text{TWAS}}=3.0\times10^{-6}$ ; *TEF*:  $P_{\text{TWAS}}=3.1\times10^{-6}$ ) and 1q31.2 (*RGS1*:  $P_{\text{TWAS}}=3.3\times10^{-6}$ ).

The TWAS recapitulated several GWAS-identified loci: 3q25.1 for EBV EBNA (*P2RY13*:  $P_{\text{cortex}}=1.1\times10^{-8}$ ; *P2RY12*:  $P_{\text{blood}}=3.3\times10^{-8}$ ) and 19q13.33 for BKV (*FUT2*:  $P_{\text{TWAS}}=8.1\times10^{-13}$ ; *NTN5*:  $P_{\text{TWAS}}=1.1\times10^{-9}$ ). Transcriptomic profiles in skin tissues provided supporting evidence for the role of multiple genes in 5q31.2 in modulating MCV antibody response (**Figure 4**; **Supplementary Table 27**). The strongest signal was observed in for *ECSCR* (skin sun unexposed:  $P_{\text{TWAS}}=5.0\times10^{-15}$ ; skin sun exposed:  $P_{\text{TWAS}}=4.2\times10^{-13}$ ), followed by *PROB1* (sun unexposed:  $P_{\text{TWAS}}=1.5\times10^{-11}$ ). *ECSCR* expression was also associated based on expression in the frontal cortex, while *PROB1* exhibited a significant, but attenuated effect in whole blood. *VWA7* was the only gene associated across all four tissues for MCV and was also associated with antibody response to several EBV antigens.

Comparison of results for seroreactivity and seropositivity revealed a number of genes implicated in both steps of the infection process (**Supplementary Table 28**). Associations with HLA DQA and DQB genes in

whole blood and HLA-DRB genes in the frontal cortex were observed for EBV antigens, JCV, and MCV. For MCV, the strongest seropositivity signals were observed for HLA class III genes *AGER* ( $P_{\text{cortex}}=9.0 \times 10^{-21}$ ) and *EHMT2* ( $P_{\text{blood}}=5.8 \times 10^{-18}$ ), which were also among the top-ranking genes for seroreactivity. Increased *ECSCR* expression conferred an increased susceptibility to MCV infection ( $P_{\text{cortex}}=1.8 \times 10^{-8}$ ), mirroring its effect on seroreactivity. In contrast to antibody response, no significant associations with any HLA genes were observed for VZV seropositivity.

Analyses using the Reactome database identified significant ( $q_{\text{FDR}} < 0.05$ ) enrichment for TWAS-identified genes in pathways involved in initiating antiviral responses, such as MHC class II antigen presentation, TCR signaling, and interferon (IFN) signaling (**Supplementary Figure 9**). Pathways unique to herpesviruses included folding, assembly and peptide loading of class I MHC ( $q=3.2 \times 10^{-7}$ ) and initial triggering of complement ( $q=9.8 \times 10^{-3}$ ). Polyomaviruses were associated with the non-canonical nuclear factor (NF)- $\kappa$ B pathway activated by tumor necrosis factor (TNF) superfamily ( $q=1.9 \times 10^{-3}$ ).

## DISCUSSION

We performed genome-wide and transcriptome-wide association studies for serological phenotypes for 16 common viruses in a well-characterized, population-based cohort. We discovered novel genetic determinants of viral antibody response beyond the HLA region for BKV, MCV, HHV7, EBV EBNA. Consistent with previous studies<sup>7,8</sup> we detected strong signals for immune response to diverse viral antigens in the HLA region, with a predominance of associations observed for alleles and amino acids in *HLA-DRB1* and *HLA-DQB1*, as well as transcriptome-level associations for multiple class II and III HLA genes. Taken together, the findings of this work provide a resource for further understanding the complex interplay between viruses and the human genome, as well as a first step towards understanding genetic determinants of reactivity to common infections.

One of our main findings is the discovery of 5q31.2 as a susceptibility locus for MCV infection and MCV antibody response, implicating two main genes: *TMEM173* (or *STING1*) and *ECSCR*. The former encodes STING (stimulator of interferon genes), an endoplasmic reticulum (ER) protein that controls the transcription of host defense genes and plays a critical role in response to DNA and RNA viruses<sup>45</sup>. STING is activated

by cyclic GMP-AMP synthase (cGAS), a cytosolic DNA sensor that mounts a response to invading pathogens by inducing IFN1 and NF- $\kappa$ B signalling<sup>46,47</sup>. Polyomaviruses penetrate the ER membrane during cell entry, a process that may be unique to this viral family<sup>48</sup>, which may trigger STING signaling in a distinct manner from other viruses<sup>48</sup>. Multiple cancer-causing viruses, such as KSHV, HBV, and HPV18, encode oncoproteins that disrupt cGAS-STING activity, which illustrates the evolutionary pressure on DNA tumor viruses to develop functions against this pathway and its importance in carcinogenesis<sup>46</sup>. Furthermore, cGAS-STING activation has been shown to trigger antitumor T-cell responses, a mechanism that can be leveraged by targeted immunotherapies<sup>49-51</sup>. Several studies suggest STING agonists may be effective against tumors resistant to PD-1 blockade, as well as promising adjuvants in cancer vaccines<sup>52-54</sup>.

*ECSCR* expression in skin and brain tissues was associated with MCV antibody response and infection. This gene encodes an endothelial cell-specific chemotaxis regulator, which plays a role in angiogenesis and apoptosis<sup>55</sup>. *ECSCR* is a negative regulator of PI3K/Akt signaling by enhancing membrane localization of *PTEN* and operates in tandem with VEGFR-2 and other receptor tyrosine kinases<sup>56</sup>. In addition to 5q31.2, another novel MCV seroreactivity associated region was identified in 3p24.3, anchored by rs776170649, which has been linked to platelet phenotypes<sup>57</sup>. These findings align with a role of platelet activation in defense against infections via degranulation-mediated release of chemokines and  $\beta$ -defensin<sup>58</sup>.

Genetic variation within Fucosyltransferase 2 (*FUT2*) has been studied extensively in the context of human infections; however, its effect on BKV seroreactivity is novel. Homozygotes for the nonsense mutation (rs601338 G>A) that inactivates the *FUT2* enzyme are unable to secrete ABO(H) histo-blood group antigens or express them on mucosal surfaces<sup>59,60</sup>. The allele which confers increased BKV antibody response (rs681343-T) is in LD ( $r^2=1.00$ ) with rs601338-A, the non-secretor allele, which confers resistance to norovirus<sup>61,62</sup>, rotavirus<sup>63</sup>, *H. pylori*<sup>64</sup>, childhood ear infection, mumps, and common colds<sup>13</sup>. However, increased susceptibility to other pathogens, such as meningococcus and pneumococcus<sup>65</sup> has also been observed in non-secretors. Isolating the underlying mechanisms for BKV response is challenging because *FUT2* is a pleiotropic locus associated with diverse phenotypes, including autoimmune and inflammatory conditions<sup>66,67</sup>, serum lipids<sup>68</sup>, B vitamins<sup>60,69</sup>, alcohol consumption<sup>70</sup>, and even certain cancers<sup>71</sup>. In addition to *FUT2* in 19q13.33, *NTN5* (netrin 5) suggests a possible link between BKV and neurological conditions.

NTN5 is primarily expressed in neuroproliferative areas, suggesting a role in adult neurogenesis, which is dysregulated in glioblastoma and Alzheimer's disease<sup>72,73</sup>.

We also report the first GWAS of serological phenotypes for HHV7. Genetic determinants of HHV7 antibody response in 6p21.32 were predominantly localized in *HLA-DQA1* and *HLA-DQB1*, with associations similar to other herpesviruses. In 11q23.3, rs75438046 maps to the 3' UTR of *CXCR5*, which controls viral infection in B-cell follicles<sup>74</sup>, and *BCL9L*, a translocation target in acute lymphoblastic leukemia<sup>75</sup> and transcriptional activator of the Wnt/ $\beta$ -catenin cancer signaling pathway<sup>76</sup>. In 17q21.32, *TBKBP1* encodes an adaptor protein that binds to TBK1 and is part of the TNF/NF- $\kappa$ B interaction network, where it regulates immune responses to infectious triggers, such as IFN1 signaling<sup>77</sup>. Interestingly, a protein interactome map recently revealed that SARS-CoV-2 nonstructural protein 13 (Nsp13) includes TBK1-TBKBP1 among its targets<sup>78</sup>. Other functions of the TBK1-TBKBP1 axis relate to tumor growth and immunosuppression through induction of PD-L1<sup>79</sup>.

Several additional genes involved in HHV7 immune response were identified in TWAS. *TEF* in 22q13.2 is an apoptotic regulator of hematopoietic progenitors with tumor promoting effects mediated by inhibition of G1/S cell cycle transition and Akt/FOXO signaling<sup>80</sup>. *RGS1* in 1q31.2 has been linked to multiple autoimmune diseases, including multiple sclerosis<sup>81</sup>, as well as poor prognosis in melanoma and diffuse large B cell lymphoma mediated by inactivation of Akt/ERK<sup>82,83</sup>.

Other genes outside of the HLA region associated with viral infection response were detected for EBV EBNA in 3q25.1. The lead variant (rs67886110) is an eQTL for *MED12L* and *P2RY12* genes, which have been linked to neurodegenerative conditions<sup>84,85</sup>. *P2RY12* and *P2RY13*, identified in TWAS, are purinergic receptor genes that regulate microglia homeostasis and have been implicated in Alzheimer's susceptibility via inflammatory and neurotrophic mechanisms<sup>85</sup>.

Considering genetic variation within the HLA region, our results confirm its pivotal role at the interface of host pathogen interactions and highlight the extensive sharing of HLA variants that mediate these interactions across virus families and antigens. Genes in this region code for cell-surface proteins that facilitate antigenic peptide presentation to immune cells that regulate responses to invading pathogens.



This region is critical for adaptive immune response but also has significant overlap with susceptibility alleles for autoimmune diseases. We identified 40 independent SNPs/indels associated with EBV (EBNA, EA-D, VCA p18, and ZEBRA), VZV, and MCV antibody response that accounted for all significant HLA associations for other phenotypes. Of the 14 conditionally independent, genome-wide significant classical alleles identified for 10 antigens, 7 were associated with multiple phenotypes. The most commonly shared HLA alleles were DRB5\*00:00, DRB1\*04:04, an known rheumatoid arthritis risk allele<sup>86</sup>, and DQB1\*02:01, associated with celiac disease risk<sup>87</sup>. Copy number deletion represented by DRB5\*00:00 may itself have a functional role in altering response by the absence of these alleles. DRB5\*00:00 also summarizes signals from multiple HLA loci, including the extended DRB5\*01:01-DRB1\*15:01-DQB1\*06:02-DQA1\*01:02 haplotype that has been implicated in the etiology of multiple autoimmune diseases and EBV EBNA IgG levels. DRB1\*15:01-DQB1\*06:02-DQA1\*01:02 is protective for type 1 diabetes<sup>88</sup>, while DRB5\*01:01-DRB15:01 confers the strongest risk for developing multiple sclerosis<sup>81</sup>. Amino acid residues in DRβ1 at positions 11, 13, 71, and 74 and in DQβ1 codon 57 represent established susceptibility loci for rheumatoid arthritis<sup>89</sup>, type 1 diabetes<sup>90</sup>, and multiple sclerosis<sup>91</sup> that exhibited strong associations with IgG levels for EBV, HHV7, VZV, JCV, and MCV antigens, and in some cases harbored the top signal of all HLA variants. Further research is needed to delineate shared genetic pathways that invoke autoimmunity and influence viral response.

Despite the predominance of association in HLA class II, several notable associations in HLA class I were detected. A\*29:02 conferred reduced MCV seroreactivity and its sequence overlaps with amino acid residues in the A α1 domain (Thr-9, Leu-62, Gln-63, Asn-77, and Met-97) that were also significantly associated with decreased MCV antibody response. This is consistent with downregulation of MHC I as a potential mechanism through which Merkel cell tumors evade immune surveillance<sup>92</sup>. The strongest residue-specific signal for EBV EA-D and VZV mapped to B-Asp-9, which is located in the peptide binding groove and tags the B\*08:01 allele, part of the HLA 8.1 ancestral haplotype. There is extensive evidence linking HLA 8.1, and B\*08:01 specifically, with autoimmune diseases<sup>93</sup> and certain cancers<sup>94,95</sup>, which may be attributed to its high cell-surface stability and increased probability of CD8+ T cell activation.



Comparison with other studies of host genetics and viral infection susceptibility shows that our results align with previously reported findings<sup>7-9,96</sup> (**Supplementary Table 29**). We replicated most associations from two of the largest GWAS of humoral immune response in European ancestry subjects by Hammer et al.<sup>7</sup> (n=2363) and Scepanovic et al.<sup>8</sup> (n=1000), including HLA SNPs, alleles, amino acids, and haplotypes linked to EBV EBNA IgG, MCV IgG and serostatus, and JCV serostatus. We also replicated two *HLA-DRB1* variants (rs477515, rs2854275) associated with EBV EBNA antibody levels in a Mexican American population<sup>9</sup>. GWAS of HPV16 L1 replicated a variant previously linked to HPV8 seropositivity (rs9357152,  $P=0.008$ )<sup>6</sup>. Some of our findings contrast with Tian et al.<sup>13</sup>, although we confirmed selected associations, such as A\*02:01 (shingles) with VZV ( $P=4.1 \times 10^{-8}$ ) and rs2596465 (mononucleosis) with EBV EBNA ( $P=3.3 \times 10^{-9}$ ) and EBV p18 ( $P=1.0 \times 10^{-12}$ ). These differences may be partly accounted for by self-reported disease status in Tian et al. which is likely to reflect symptom severity and may be an imprecise indicator of infection with certain viruses or the magnitude of antibody response to infection.

One of the most striking findings in SNP-based HLA analyses was the genome-wide significant association between rs9273325, index VZV antibody response variant, and risk of schizophrenia. Previous epidemiologic and serologic studies have linked infections to schizophrenia, although the underlying mechanisms remain to be elucidated<sup>97</sup>. Viruses are plausible etiologic candidates for schizophrenia due to their ability to invade the central nervous system and disrupt neurodevelopmental processes by targeting specific neurons, as well as the potential for latent infection to negatively impact plasticity and neurogenesis via pro-inflammatory and aberrant immune signaling<sup>97,98</sup>. These observations are consistent with the established role the HLA region, including *HLA-DQB1*, in schizophrenia etiology<sup>99,100</sup>, and is further supported by previously reported associations for rs9273325 with blood cell traits<sup>57</sup> and immunoglobulin A deficiency<sup>101</sup>, as well as its role as an eQTL for *HLA-DQB1* in CD4+ T<sub>H</sub> cells. Schizophrenia susceptibility alleles DRB1\*03:01<sup>99</sup>, DQB1\*02:01, and B\*08:01 were also the top three alleles associated with VZV antibody response in the unconditional analysis. Enhanced complement activity has been proposed as the mechanism mediating the synaptic loss and excessive pruning which is a hallmark of schizophrenia pathophysiology<sup>102</sup>. Complement component 4 (C4) alleles were found to increase risk of schizophrenia proportionally to their effect on increasing *C4A* expression in brain tissue<sup>102</sup>. Using gene expression models in whole blood and the frontal cortex we demonstrated that increased *C4A* expression is negatively

associated with VZV antibody response. We also observed associations with *C4A* and *C4B* in EBV and HSV-1, but not other viruses. Taken together, these findings delineate a potential mechanism through which aberrant immune response to VZV infection, and potentially HSV-1 and EBV, may increase susceptibility to schizophrenia. However, cautious interpretation is warranted due to significant pleiotropy between HLA loci associated with viral infection and broad immune function.

Several limitations of this work should be noted. First, the UK Biobank is unrepresentative of the general UK population due to low participation resulting in healthy volunteer bias<sup>103</sup>. However, since the observed pattern of seroprevalence is consistent with previously published estimates<sup>15</sup> we believe the impact of this bias is likely to be minimal on genetic associations with serological phenotypes. Second, our analyses were restricted to participants of European ancestry due to limited serology data for other ancestries, which limits the generalizability of our findings to diverse populations. Third, we were unable to conduct formal statistical replication of novel GWAS and TWAS signals in an independent sample due to the lack of such a population. Nevertheless, our successful replication of multiple previously reported variants and, combined with the observation that newly discovered genes and variants are part of essential adaptive and innate immunity pathways, support the credibility of our findings. Lastly, we also stress caution in the interpretation of GWAS results for non-ubiquitous pathogens, such as HBV, HCV, and HPV, due to a lack of information on exposure, as well as low numbers of seropositive individuals.

Our study also has distinct advantages. The large sample size of the UK Biobank facilitated more powerful genetic association analyses than previous studies, particularly in a population-based cohort unselected for disease status. Our detailed HLA analysis shows independent effects of specific HLA alleles and pleiotropic effects across multiple viruses. Analyses of genetic associations in external datasets further demonstrate a connection between host genetic factors influencing immune response to infection and susceptibility to cancers and neurological conditions.

The results of this work highlight widespread genetic pleiotropy between pathways involved in regulating humoral immune response to novel and common viruses, as well as complex diseases. The complex evolutionary relationship between viruses and humans is not dictated simply by infection and acute sickness, it is a complex nuanced architecture of initial challenge tempered with tolerance of viral latency

527 over time. Yet it is that architecture that is evolutionarily optimized to maximize fitness early in life, the result  
528 of which may be increased risk for complex diseases later in life. Understanding this complex interplay  
529 through both targeted association studies and functional investigations between host genetic factors and  
530 immune response has implications for complex disease etiology and may facilitate the discovery of novel  
531 therapeutics in a wide range of diseases.

## DATA AVAILABILITY

The UK Biobank is an open access resource, available at <https://www.ukbiobank.ac.uk/researchers/>. This research was conducted with approved access to UK Biobank data under application number 14105 (PI: Witte).

## WEB RESOURCES

PLINK 2.0: <https://www.cog-genomics.org/plink/2.0/>  
 PLINK 1.07 conditional haplotype module: <https://zzz.bwh.harvard.edu/plink/whap.shtml>  
 R packages for pathway analysis: <https://bioconductor.org/packages/release/bioc/html/ReactomePA.html>  
 and <https://bioconductor.org/packages/release/bioc/html/clusterProfiler.html>  
 Database of HLA allele frequencies and amino acid substitutions:  
[http://www.allelefrequencies.net/hla9001a.asp?type\\_analysis=by\\_pops](http://www.allelefrequencies.net/hla9001a.asp?type_analysis=by_pops)

## ACKNOWLEDGEMENTS

This research was supported by funding from the National Institutes of Health (US NCI R25T CA112355 and R01 CA201358; PI: Witte). Maïke Morrison was funded by the University of California San Francisco's Amgen Scholars Program.

## COMPETING INTERESTS

The authors declare no competing interests.

## References

1. Aiweesakun, P. & Katzourakis, A. Marine origin of retroviruses in the early Palaeozoic Era. *Nat Commun* **8**, 13954 (2017).
2. Wang, W. *et al.* Detection of SARS-CoV-2 in Different Types of Clinical Specimens. *JAMA* (2020).
3. Moore, P.S. & Chang, Y. Why do viruses cause cancer? Highlights of the first century of human tumour virology. *Nat Rev Cancer* **10**, 878-89 (2010).
4. Engdahl, E. *et al.* Increased Serological Response Against Human Herpesvirus 6A Is Associated With Risk for Multiple Sclerosis. *Front Immunol* **10**, 2715 (2019).
5. Readhead, B. *et al.* Multiscale Analysis of Independent Alzheimer's Cohorts Finds Disruption of Molecular, Genetic, and Clinical Networks by Human Herpesvirus. *Neuron* **99**, 64-82 e7 (2018).
6. Chen, D. *et al.* Genome-wide association study of HPV seropositivity. *Hum Mol Genet* **20**, 4714-23 (2011).
7. Hammer, C. *et al.* Amino Acid Variation in HLA Class II Proteins Is a Major Determinant of Humoral Response to Common Viruses. *Am J Hum Genet* **97**, 738-43 (2015).
8. Scepanovic, P. *et al.* Human genetic variants and age are the strongest predictors of humoral immune responses to common pathogens and vaccines. *Genome Med* **10**, 59 (2018).
9. Rubicz, R. *et al.* A genome-wide integrative genomic study localizes genetic factors influencing antibodies against Epstein-Barr virus nuclear antigen 1 (EBNA-1). *PLoS Genet* **9**, e1003147 (2013).
10. Liu, S. *et al.* Genomic Analyses from Non-invasive Prenatal Testing Reveal Genetic Associations, Patterns of Viral Infections, and Chinese Population History. *Cell* **175**, 347-359 e14 (2018).
11. Besson, C. *et al.* Strong correlations of anti-viral capsid antigen antibody levels in first-degree relatives from families with Epstein-Barr virus-related lymphomas. *J Infect Dis* **199**, 1121-7 (2009).
12. Kenney, A.D. *et al.* Human Genetic Determinants of Viral Diseases. *Annu Rev Genet* **51**, 241-263 (2017).
13. Tian, C. *et al.* Genome-wide association and HLA region fine-mapping studies identify susceptibility loci for multiple common infections. *Nat Commun* **8**, 599 (2017).
14. Bycroft, C. *et al.* The UK Biobank resource with deep phenotyping and genomic data. *Nature* **562**, 203-209 (2018).
15. Mentzer, A.J. *et al.* Identification of host-pathogen-disease relationships using a scalable Multiplex Serology platform in UK Biobank. *medRxiv*, 19004960 (2019).
16. Manichaikul, A. *et al.* Robust relationship inference in genome-wide association studies. *Bioinformatics* **26**, 2867-73 (2010).
17. Waterboer, T. *et al.* Multiplex human papillomavirus serology based on in situ-purified glutathione s-transferase fusion proteins. *Clin Chem* **51**, 1845-53 (2005).
18. Waterboer, T., Sehr, P. & Pawlita, M. Suppression of non-specific binding in serological Luminex assays. *J Immunol Methods* **309**, 200-4 (2006).

19. Kreimer, A.R. *et al.* Kinetics of the Human Papillomavirus Type 16 E6 Antibody Response Prior to Oropharyngeal Cancer. *J Natl Cancer Inst* **109**(2017).
20. Peterson, R.A. & Cavanaugh, J.E. Ordered quantile normalization: a semiparametric transformation built for the cross-validation era. *Journal of Applied Statistics*, 1-16 (2019).
21. Rentzsch, P., Witten, D., Cooper, G.M., Shendure, J. & Kircher, M. CADD: predicting the deleteriousness of variants throughout the human genome. *Nucleic Acids Res* **47**, D886-D894 (2019).
22. Dong, S. & Boyle, A.P. Predicting functional variants in enhancer and promoter elements using RegulomeDB. *Hum Mutat* **40**, 1292-1298 (2019).
23. Schmiedel, B.J. *et al.* Impact of Genetic Polymorphisms on Human Immune Cell Gene Expression. *Cell* **175**, 1701-1715 e16 (2018).
24. Sun, B.B. *et al.* Genomic atlas of the human plasma proteome. *Nature* **558**, 73-79 (2018).
25. Yao, C. *et al.* Genome-wide mapping of plasma protein QTLs identifies putatively causal genes and pathways for cardiovascular disease. *Nat Commun* **9**, 3268 (2018).
26. Rashkin, S.R. *et al.* Pan-Cancer Study Detects Novel Genetic Risk Variants and Shared Genetic Basis in Two Large Cohorts. *bioRxiv*, 635367 (2019).
27. Lam, M. *et al.* Comparative genetic architectures of schizophrenia in East Asian and European populations. *Nat Genet* **51**, 1670-1678 (2019).
28. Jun, G. *et al.* A novel Alzheimer disease locus located near the gene encoding tau protein. *Mol Psychiatry* **21**, 108-17 (2016).
29. Motyer, A. *et al.* Practical Use of Methods for Imputation of HLA Alleles from SNP Genotype Data. *bioRxiv*, 091009 (2016).
30. Jia, X. *et al.* Imputing amino acid polymorphisms in human leukocyte antigens. *PLoS One* **8**, e64683 (2013).
31. Gonzalez-Galarza, F.F. *et al.* Allele frequency net database (AFND) 2020 update: gold-standard data classification, open access genotype data and new query tools. *Nucleic Acids Res* **48**, D783-D788 (2020).
32. Barbeira, A.N. *et al.* Exploring the phenotypic consequences of tissue specific gene expression variation inferred from GWAS summary statistics. *Nat Commun* **9**, 1825 (2018).
33. Barbeira, A.N. *et al.* Widespread dose-dependent effects of RNA expression and splicing on complex diseases and traits. *bioRxiv*, 814350 (2019).
34. Urbut, S.M., Wang, G., Carbonetto, P. & Stephens, M. Flexible statistical methods for estimating and testing effects in genomic studies with multiple conditions. *Nat Genet* **51**, 187-195 (2019).
35. Wen, X., Lee, Y., Luca, F. & Pique-Regi, R. Efficient Integrative Multi-SNP Association Analysis via Deterministic Approximation of Posteriors. *Am J Hum Genet* **98**, 1114-1129 (2016).
36. Lee, Y., Luca, F., Pique-Regi, R. & Wen, X. Bayesian Multi-SNP Genetic Association Analysis: Control of FDR and Use of Summary Statistics. *bioRxiv*, 316471 (2018).

37. Steiner, I., Kennedy, P.G. & Pachner, A.R. The neurotropic herpes viruses: herpes simplex and varicella-zoster. *Lancet Neurol* **6**, 1015-28 (2007).
38. Khalili, K., Del Valle, L., Otte, J., Weaver, M. & Gordon, J. Human neurotropic polyomavirus, JCV, and its role in carcinogenesis. *Oncogene* **22**, 5181-91 (2003).
39. Feng, H., Shuda, M., Chang, Y. & Moore, P.S. Clonal integration of a polyomavirus in human Merkel cell carcinoma. *Science* **319**, 1096-100 (2008).
40. Szklarczyk, D. *et al.* STRING v11: protein-protein association networks with increased coverage, supporting functional discovery in genome-wide experimental datasets. *Nucleic Acids Res* **47**, D607-D613 (2019).
41. Shin, O.S. *et al.* LPLUNC1 modulates innate immune responses to *Vibrio cholerae*. *J Infect Dis* **204**, 1349-57 (2011).
42. Shafi, O. Inverse relationship between Alzheimer's disease and cancer, and other factors contributing to Alzheimer's disease: a systematic review. *BMC Neurol* **16**, 236 (2016).
43. Gragert, L., Madbouly, A., Freeman, J. & Maier, M. Six-locus high resolution HLA haplotype frequencies derived from mixed-resolution DNA typing for the entire US donor registry. *Hum Immunol* **74**, 1313-20 (2013).
44. Degenhardt, F. *et al.* Construction and benchmarking of a multi-ethnic reference panel for the imputation of HLA class I and II alleles. *Hum Mol Genet* **28**, 2078-2092 (2019).
45. Chen, Q., Sun, L. & Chen, Z.J. Regulation and function of the cGAS-STING pathway of cytosolic DNA sensing. *Nat Immunol* **17**, 1142-9 (2016).
46. Kwon, J. & Bakhom, S.F. The Cytosolic DNA-Sensing cGAS-STING Pathway in Cancer. *Cancer Discov* **10**, 26-39 (2020).
47. Sun, L., Wu, J., Du, F., Chen, X. & Chen, Z.J. Cyclic GMP-AMP synthase is a cytosolic DNA sensor that activates the type I interferon pathway. *Science* **339**, 786-91 (2013).
48. Inoue, T. & Tsai, B. How viruses use the endoplasmic reticulum for entry, replication, and assembly. *Cold Spring Harb Perspect Biol* **5**, a013250 (2013).
49. Woo, S.R. *et al.* STING-dependent cytosolic DNA sensing mediates innate immune recognition of immunogenic tumors. *Immunity* **41**, 830-42 (2014).
50. Demaria, O. *et al.* STING activation of tumor endothelial cells initiates spontaneous and therapeutic antitumor immunity. *Proc Natl Acad Sci U S A* **112**, 15408-13 (2015).
51. Ohkuri, T. *et al.* STING contributes to antiglioma immunity via triggering type I IFN signals in the tumor microenvironment. *Cancer Immunol Res* **2**, 1199-208 (2014).
52. Fu, J. *et al.* STING agonist formulated cancer vaccines can cure established tumors resistant to PD-1 blockade. *Sci Transl Med* **7**, 283ra52 (2015).
53. Corrales, L. *et al.* Direct Activation of STING in the Tumor Microenvironment Leads to Potent and Systemic Tumor Regression and Immunity. *Cell Rep* **11**, 1018-30 (2015).



54. Ohkuri, T., Ghosh, A., Kosaka, A., Sarkar, S.N. & Okada, H. Protective role of STING against gliomagenesis: Rational use of STING agonist in anti-glioma immunotherapy. *Oncoimmunology* **4**, e999523 (2015).
55. Ikeda, K. *et al.* Identification of ARIA regulating endothelial apoptosis and angiogenesis by modulating proteasomal degradation of cIAP-1 and cIAP-2. *Proc Natl Acad Sci U S A* **106**, 8227-32 (2009).
56. Verma, A. *et al.* Endothelial cell-specific chemotaxis receptor (ecscr) promotes angioblast migration during vasculogenesis and enhances VEGF receptor sensitivity. *Blood* **115**, 4614-22 (2010).
57. Astle, W.J. *et al.* The Allelic Landscape of Human Blood Cell Trait Variation and Links to Common Complex Disease. *Cell* **167**, 1415-1429 e19 (2016).
58. Assinger, A. Platelets and infection - an emerging role of platelets in viral infection. *Front Immunol* **5**, 649 (2014).
59. Kelly, R.J., Rouquier, S., Giorgi, D., Lennon, G.G. & Lowe, J.B. Sequence and expression of a candidate for the human Secretor blood group alpha(1,2)fucosyltransferase gene (FUT2). Homozygosity for an enzyme-inactivating nonsense mutation commonly correlates with the non-secretor phenotype. *J Biol Chem* **270**, 4640-9 (1995).
60. Hazra, A. *et al.* Common variants of FUT2 are associated with plasma vitamin B12 levels. *Nat Genet* **40**, 1160-2 (2008).
61. Carlsson, B. *et al.* The G428A nonsense mutation in FUT2 provides strong but not absolute protection against symptomatic GII.4 Norovirus infection. *PLoS One* **4**, e5593 (2009).
62. Ruvoen-Clouet, N., Belliot, G. & Le Pendu, J. Noroviruses and histo-blood groups: the impact of common host genetic polymorphisms on virus transmission and evolution. *Rev Med Virol* **23**, 355-66 (2013).
63. Imbert-Marcille, B.M. *et al.* A FUT2 gene common polymorphism determines resistance to rotavirus A of the P[8] genotype. *J Infect Dis* **209**, 1227-30 (2014).
64. Ikehara, Y. *et al.* Polymorphisms of two fucosyltransferase genes (Lewis and Secretor genes) involving type I Lewis antigens are associated with the presence of anti-Helicobacter pylori IgG antibody. *Cancer Epidemiol Biomarkers Prev* **10**, 971-7 (2001).
65. Blackwell, C.C. *et al.* Non-secretion of ABO antigens predisposing to infection by Neisseria meningitidis and Streptococcus pneumoniae. *Lancet* **2**, 284-5 (1986).
66. de Lange, K.M. *et al.* Genome-wide association study implicates immune activation of multiple integrin genes in inflammatory bowel disease. *Nat Genet* **49**, 256-261 (2017).
67. Ellinghaus, D. *et al.* Analysis of five chronic inflammatory diseases identifies 27 new associations and highlights disease-specific patterns at shared loci. *Nat Genet* **48**, 510-8 (2016).
68. Hoffmann, T.J. *et al.* A large electronic-health-record-based genome-wide study of serum lipids. *Nat Genet* **50**, 401-413 (2018).



69. Tanaka, T. *et al.* Genome-wide association study of vitamin B6, vitamin B12, folate, and homocysteine blood concentrations. *Am J Hum Genet* **84**, 477-82 (2009).
70. Liu, M. *et al.* Association studies of up to 1.2 million individuals yield new insights into the genetic etiology of tobacco and alcohol use. *Nat Genet* **51**, 237-244 (2019).
71. McKay, J.D. *et al.* Large-scale association analysis identifies new lung cancer susceptibility loci and heterogeneity in genetic susceptibility across histological subtypes. *Nat Genet* **49**, 1126-1132 (2017).
72. Batista, C.M. *et al.* Adult neurogenesis and glial oncogenesis: when the process fails. *Biomed Res Int* **2014**, 438639 (2014).
73. Yamagishi, S. *et al.* Netrin-5 is highly expressed in neurogenic regions of the adult brain. *Front Cell Neurosci* **9**, 146 (2015).
74. Leong, Y.A. *et al.* CXCR5(+) follicular cytotoxic T cells control viral infection in B cell follicles. *Nat Immunol* **17**, 1187-96 (2016).
75. Willis, T.G. *et al.* Molecular cloning of translocation t(1;14)(q21;q32) defines a novel gene (BCL9) at chromosome 1q21. *Blood* **91**, 1873-81 (1998).
76. Deka, J. *et al.* Bcl9/Bcl9l are critical for Wnt-mediated regulation of stem cell traits in colon epithelium and adenocarcinomas. *Cancer Res* **70**, 6619-28 (2010).
77. Pilli, M. *et al.* TBK-1 promotes autophagy-mediated antimicrobial defense by controlling autophagosome maturation. *Immunity* **37**, 223-34 (2012).
78. Gordon, D.E. *et al.* A SARS-CoV-2 protein interaction map reveals targets for drug repurposing. *Nature* (2020).
79. Zhu, L. *et al.* TBKBP1 and TBK1 form a growth factor signalling axis mediating immunosuppression and tumorigenesis. *Nat Cell Biol* **21**, 1604-1614 (2019).
80. Yang, J. *et al.* Thyrotroph embryonic factor is downregulated in bladder cancer and suppresses proliferation and tumorigenesis via the AKT/FOXOs signalling pathway. *Cell Prolif* **52**, e12560 (2019).
81. International Multiple Sclerosis Genetics, C. *et al.* Genetic risk and a primary role for cell-mediated immune mechanisms in multiple sclerosis. *Nature* **476**, 214-9 (2011).
82. Sun, M.Y. *et al.* Critical role for nonGAP function of Galphas in RGS1mediated promotion of melanoma progression through AKT and ERK phosphorylation. *Oncol Rep* **39**, 2673-2680 (2018).
83. Carreras, J. *et al.* Clinicopathological characteristics and genomic profile of primary sinonasal tract diffuse large B cell lymphoma (DLBCL) reveals gain at 1q31 and RGS1 encoding protein; high RGS1 immunohistochemical expression associates with poor overall survival in DLBCL not otherwise specified (NOS). *Histopathology* **70**, 595-621 (2017).
84. Mukherjee, S. *et al.* Genetic data and cognitively defined late-onset Alzheimer's disease subgroups. *Mol Psychiatry* (2018).

85. Keren-Shaul, H. *et al.* A Unique Microglia Type Associated with Restricting Development of Alzheimer's Disease. *Cell* **169**, 1276-1290 e17 (2017).
86. Jawaheer, D. *et al.* Dissecting the genetic complexity of the association between human leukocyte antigens and rheumatoid arthritis. *Am J Hum Genet* **71**, 585-94 (2002).
87. Vader, W. *et al.* The HLA-DQ2 gene dose effect in celiac disease is directly related to the magnitude and breadth of gluten-specific T cell responses. *Proc Natl Acad Sci U S A* **100**, 12390-5 (2003).
88. Erlich, H. *et al.* HLA DR-DQ haplotypes and genotypes and type 1 diabetes risk: analysis of the type 1 diabetes genetics consortium families. *Diabetes* **57**, 1084-92 (2008).
89. Raychaudhuri, S. *et al.* Five amino acids in three HLA proteins explain most of the association between MHC and seropositive rheumatoid arthritis. *Nat Genet* **44**, 291-6 (2012).
90. Hu, X. *et al.* Additive and interaction effects at three amino acid positions in HLA-DQ and HLA-DR molecules drive type 1 diabetes risk. *Nat Genet* **47**, 898-905 (2015).
91. Patsopoulos, N.A. *et al.* Fine-mapping the genetic association of the major histocompatibility complex in multiple sclerosis: HLA and non-HLA effects. *PLoS Genet* **9**, e1003926 (2013).
92. Paulson, K.G. *et al.* Downregulation of MHC-I expression is prevalent but reversible in Merkel cell carcinoma. *Cancer Immunol Res* **2**, 1071-9 (2014).
93. Candore, G., Lio, D., Colonna Romano, G. & Caruso, C. Pathogenesis of autoimmune diseases associated with 8.1 ancestral haplotype: effect of multiple gene interactions. *Autoimmun Rev* **1**, 29-35 (2002).
94. Ferreira-Iglesias, A. *et al.* Fine mapping of MHC region in lung cancer highlights independent susceptibility loci by ethnicity. *Nat Commun* **9**, 3927 (2018).
95. Abdou, A.M. *et al.* Human leukocyte antigen (HLA) A1-B8-DR3 (8.1) haplotype, tumor necrosis factor (TNF) G-308A, and risk of non-Hodgkin lymphoma. *Leukemia* **24**, 1055-8 (2010).
96. Sundqvist, E. *et al.* JC polyomavirus infection is strongly controlled by human leukocyte antigen class II variants. *PLoS Pathog* **10**, e1004084 (2014).
97. Khandaker, G.M. *et al.* Inflammation and immunity in schizophrenia: implications for pathophysiology and treatment. *Lancet Psychiatry* **2**, 258-270 (2015).
98. Dickerson, F. *et al.* Schizophrenia is Associated With an Aberrant Immune Response to Epstein-Barr Virus. *Schizophr Bull* **45**, 1112-1119 (2019).
99. International Schizophrenia, C. *et al.* Common polygenic variation contributes to risk of schizophrenia and bipolar disorder. *Nature* **460**, 748-52 (2009).
100. Schizophrenia Working Group of the Psychiatric Genomics, C. Biological insights from 108 schizophrenia-associated genetic loci. *Nature* **511**, 421-7 (2014).
101. Bronson, P.G. *et al.* Common variants at PVT1, ATG13-AMBRA1, AHI1 and CLEC16A are associated with selective IgA deficiency. *Nat Genet* **48**, 1425-1429 (2016).
102. Sekar, A. *et al.* Schizophrenia risk from complex variation of complement component 4. *Nature* **530**, 177-83 (2016).

770 103. Fry, A. *et al.* Comparison of Sociodemographic and Health-Related Characteristics of UK Biobank  
771 Participants With Those of the General Population. *Am J Epidemiol* **186**, 1026-1034 (2017).  
772

**Table 1:** Lead genome-wide significant variants ( $P < 5.0 \times 10^{-8}$ ) for continuous antibody response phenotypes for antigens with at least 20% seroprevalence.

Antigen		N	Chr	Position	Variant	Alleles Effect Other		EAF	Beta <sup>2</sup>	(SE)	P	Function	Nearest Gene
CMV	pp52	5000	6	32301427	rs115378818	C	T	0.978	0.633	(0.095)	$2.9 \times 10^{-11}$	intronic	<i>TSBP1</i>
EBV	EA-D	6806	6	32665840	rs34825357	T	TC	0.409	-0.114	(0.017)	$2.0 \times 10^{-11}$	intergenic	<i>MTCO3P1</i>
EBV	EBNA	7003	3	151114852	rs67886110*	G	T	0.596	0.103	(0.017)	$1.3 \times 10^{-9}$	intronic	<i>MED12L</i>
			6	32451762	rs9269233	A	C	0.249	0.315	(0.019)	$3.5 \times 10^{-61}$	intergenic	<i>HLA-DRB9</i>
EBV	VCA p18	7492	6	31486158	6:31486158	GT	G	0.245	0.197	(0.018)	$7.1 \times 10^{-27}$	intergenic	<i>PPIAP9</i>
EBV	ZEBRA	7197	6	32637772	rs9274728	A	G	0.718	-0.315	(0.018)	$4.7 \times 10^{-67}$	intergenic	<i>HLA-DQB1</i>
HHV6	IE1A	6077	7	139985625	rs2429218	T	C	0.615	0.106	(0.019)	$1.4 \times 10^{-8}$	downstream	<i>RP5-1136G2.1</i>
			6	32602665	rs139299944	C	CT	0.655	0.114	(0.017)	$1.5 \times 10^{-11}$	intronic	<i>HLA-DQA1</i>
HHV7	U14	7481	11	118767564	rs75438046	G	A	0.970	0.280	(0.049)	$1.3 \times 10^{-8}$	3'-UTR	<i>CXCR5 / BCL9L</i>
			17	45794706	rs1808192	A	G	0.331	-0.099	(0.017)	$9.8 \times 10^{-9}$	intergenic	<i>TBKBP1</i>
HSV1	1gG	5468	6	32627852	rs1130420	G	A	0.583	-0.122	(0.019)	$2.5 \times 10^{-10}$	3'-UTR	<i>HLA-DQB1</i>
			10	91189187	rs11203123*	A	C	0.988	0.512	(0.093)	$3.9 \times 10^{-8}$	intergenic	<i>SLC16A12</i>
VZV	gE/Ig <sup>1</sup>	7289	6	32623193	rs9273325	G	A	0.831	-0.232	(0.021)	$8.2 \times 10^{-28}$	intergenic	<i>HLA-DQB1</i>
BKV	VP1	7523	19	49206462	rs681343	C	T	0.491	-0.125	(0.016)	$4.7 \times 10^{-15}$	synonymous	<i>FUT2</i>
JCV	VP1	4471	6	32589842	rs9271525	G	A	0.163	-0.318	(0.031)	$3.9 \times 10^{-24}$	intergenic	<i>HLA-DQA1</i>
			3	18238783	rs776170649	CT	C	0.790	-0.134	(0.024)	$1.7 \times 10^{-8}$	intergenic	<i>LOC339862</i>
MCV	VP1	5219	5	138865423	rs7444313	G	A	0.263	0.169	(0.021)	$2.4 \times 10^{-15}$	intergenic	<i>TMEM173</i>
			6	32429277	rs9268847	A	G	0.750	-0.195	(0.022)	$2.4 \times 10^{-19}$	intronic	<i>HLA-DRB9</i>

<sup>1</sup> VZV antigens gE and gI were co-loaded onto the same Luminex bead set

<sup>2</sup> Regression coefficients were estimated per 1 standard deviation increase in normalized MFI value z-scores with adjustment for age at enrollment, sex, body mass index, socioeconomic status (Townsend deprivation index), the presence of any autoimmune conditions, genotyping array, serology assay date, quality control flag and the top 10 genetic ancestry principal components

\* Multi-allelic variants: rs67886110 (G/T and G/C) and rs11203123 (A/C and A/AC)

**Figure 1:** Flow chart describing the main serological phenotypes and association analyses

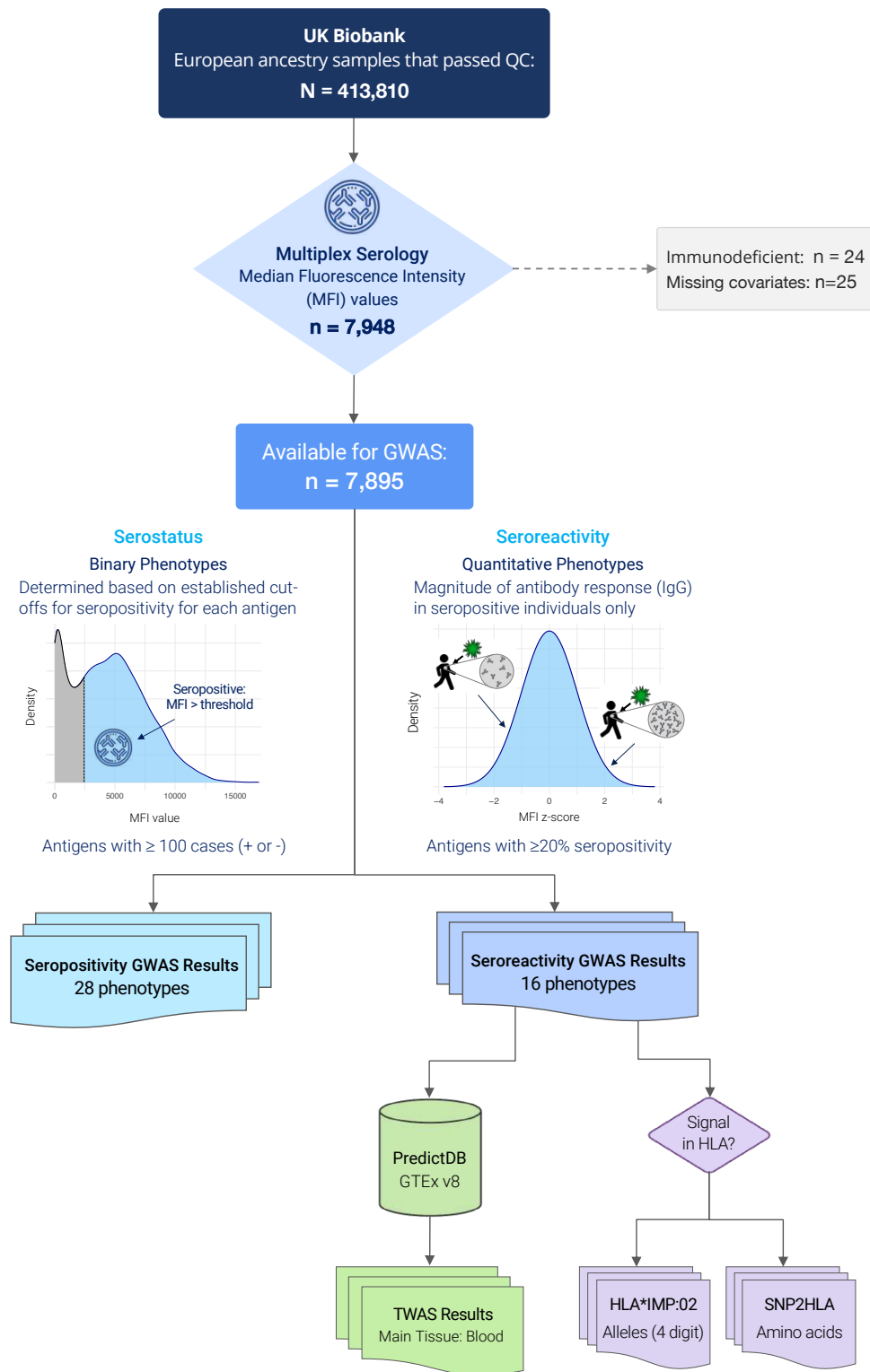


**Figure 2:** Results from genome-wide and regional association analyses of continuous antibody response phenotypes (MFI z-scores) among individuals seropositive for human polyomaviruses BKV, JCV, and Merkel cell (MCV). The lower two panels depict the association signal and linkage disequilibrium (LD) structure in the HLA region for JCV and MCV.

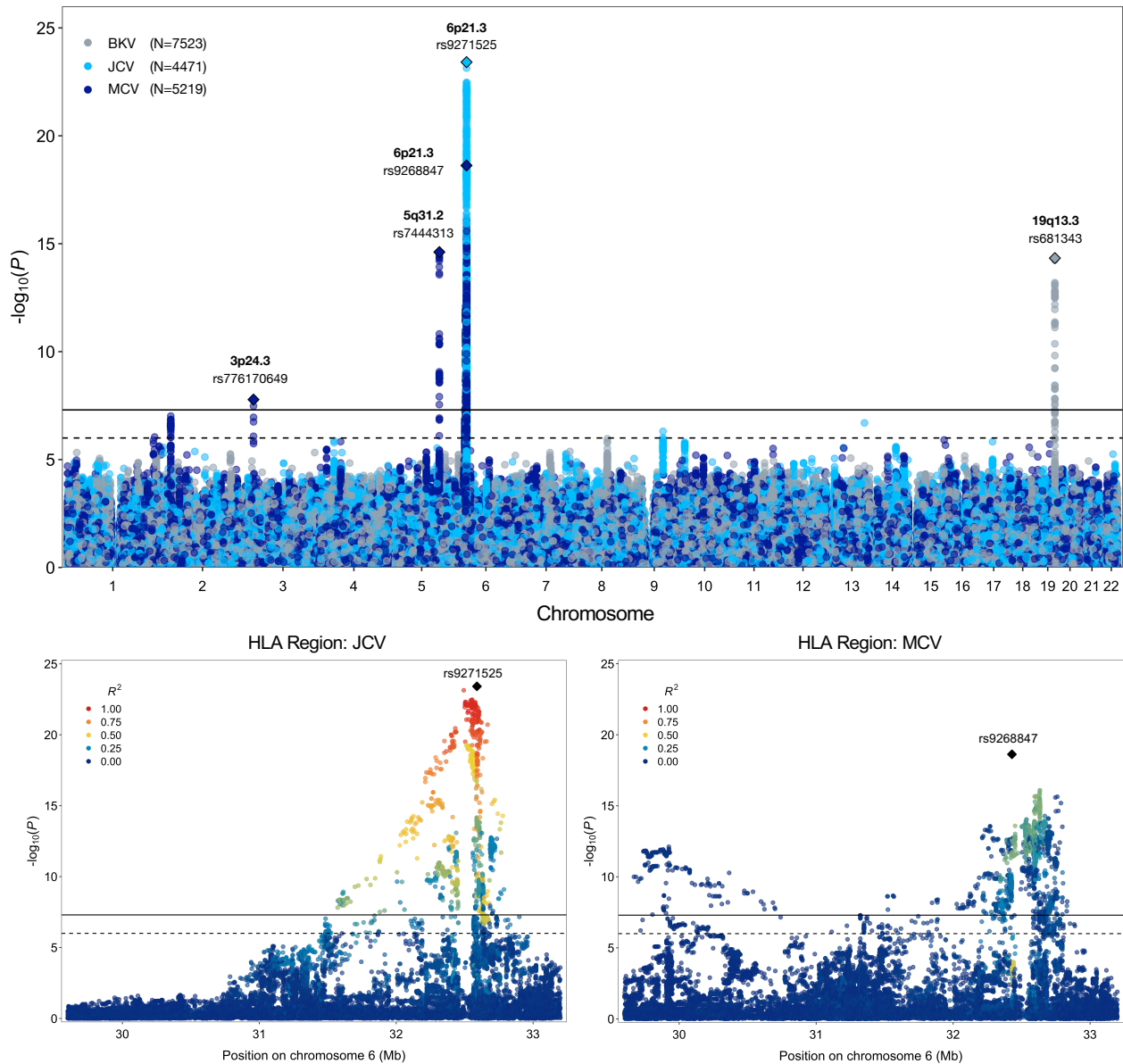


**Figure 3:** Regional association plots for conditionally independent HLA genetic variants that were significantly ( $P < 5.0 \times 10^{-8}$ , solid black line) associated with each continuous antibody response phenotype. The suggestive significance threshold corresponds to  $P < 1.0 \times 10^{-6}$  (dotted black line).

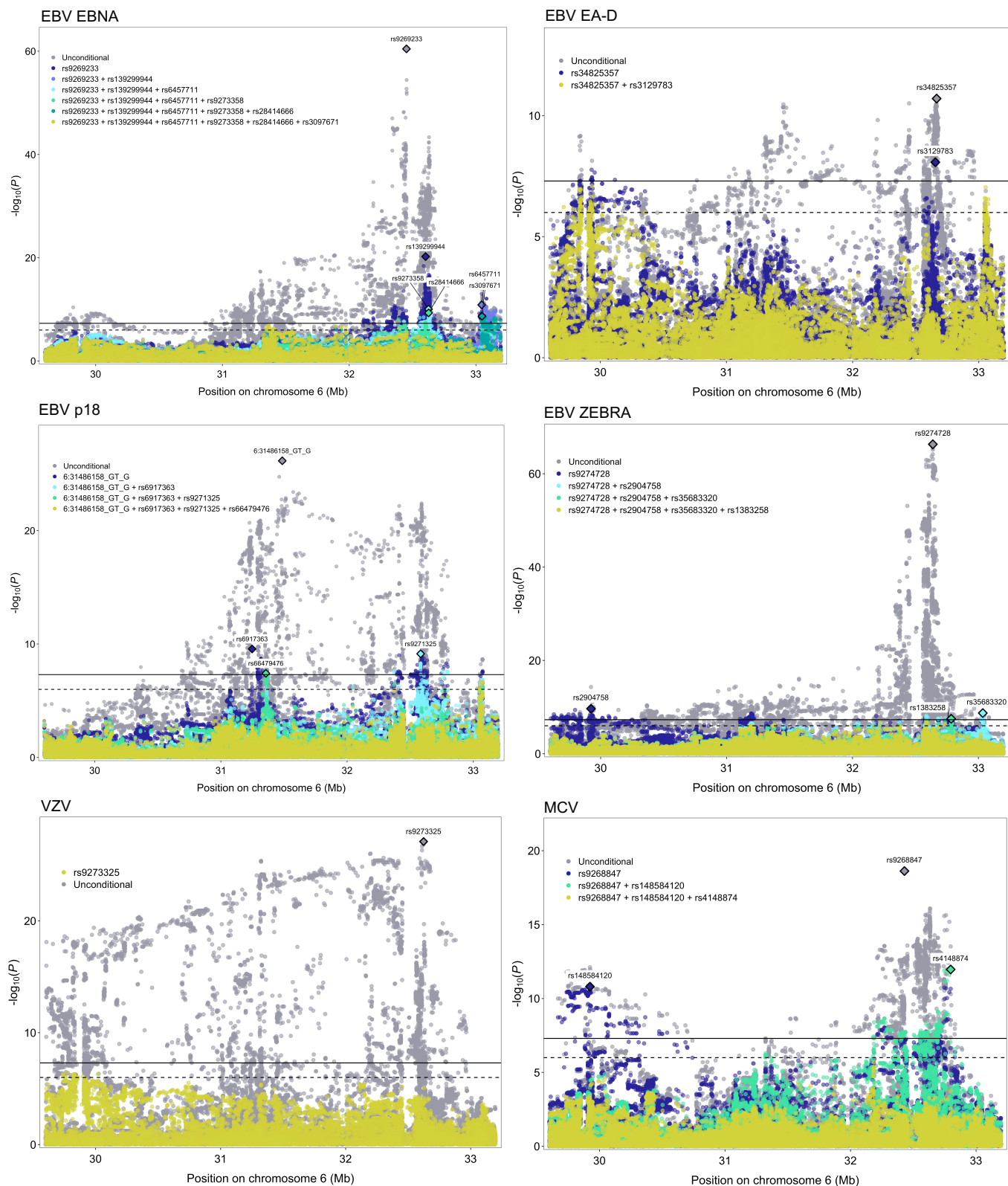
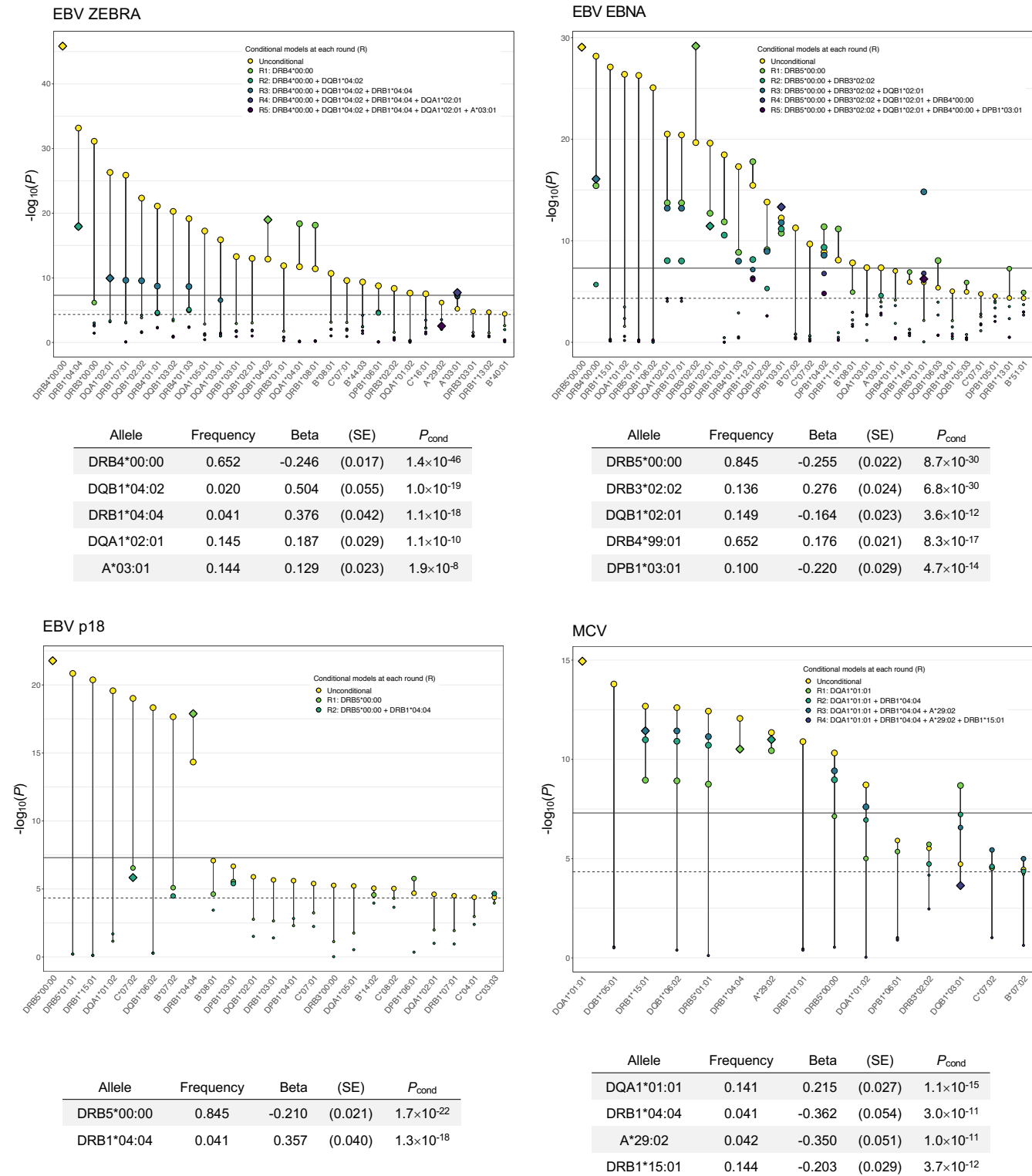




**Figure 4:** Conditionally independent classical HLA alleles significantly ( $P_{\text{cond}} < 5.0 \times 10^{-8}$ , solid line) associated with each continuous antibody response phenotype. Only classical alleles that surpassed the Bonferroni-corrected significance threshold ( $P < 4.6 \times 10^{-5}$ , dotted line) were included in conditional analyses.





VZV

$-\log_{10}(P)$

Chromosome

1 2 3 4 5 6 7 8 9 10 11 12 13 14 15 16 17 18 19 20 21 22

20

10

0

-10

-20

GY2P1A2

C4B

C4A

AGER

HCP5B

LIN28B

ZKSCAN4

ZFP57

OR2H3

ZKSCAN5

GABRR1

CSNK2B

HLA-DMA

BAG6

GCHCR1

MUC8

HLA-DQB2

U01328.10

HSPA1B

PPT2

RP1-86C11.1

VWA7

HIST1H2BC

ZSCAN5

HLA-A

P3X2

ZSCAN12

ZSCAN36

BTNGA2

TRIM10

C4A

GLIC

APOH1

NEU1

